Transition between Quantum States in a Parallel-Coupled Double Quantum Dot

J. C. Chen,[1] A. M. Chang,[1,*] and M. R. Melloch[2]

[1]*Department of Physics, Purdue University, West Lafayette, Indiana 47907, USA*

[2]*School of Electrical and Computer Engineering, Purdue University, West Lafayette, Indiana 47907, USA*

(Received 12 May 2003; published 27 April 2004)

Strong electron and spin correlations in a double quantum dot (DQD) can give rise to different quantum states. We observe a continuous transition from a Kondo state exhibiting a single-peak Kondo resonance to another exhibiting a double peak by increasing the interdot coupling (t) in a parallel-coupled DQD. The transition into the double-peak state provides evidence for spin entanglement between the excess electrons on each dot. Toward the transition, the peak splitting merges and becomes substantially smaller than t because of strong Coulomb effects. Our device tunability bodes well for future quantum computation applications.

DOI: 10.1103/PhysRevLett.92.176801 PACS numbers: 73.23.–b, 73.63.Kv

The double quantum dot (DQD) is emerging as a versatile system for studying a variety of strongly correlated behaviors [1–7]. Following the experimental demonstration of the Kondo impurity-spin screening effect in single quantum dots [8–13], recent theoretical investigations of the coupled DQD system is uncovering new correlated behaviors [1–7]. These works suggest that the DQD enables a realization of the two-impurity Kondo problem first discussed in the context of metallic systems [1,14–16] in which a competition between Kondo correlations and antiferromagnetic (AF) impurity-spin correlation leads to a quantum critical phenomenon. In a different regime of parameters, a related quantum critical phenomenon can occur driven by a competition between intradot Kondo coupling to leads and the interdot coupling [2,3]. In each scenario, a transition is predicted to occur between a quantum state characterized by a single-peaked Kondo resonance, and a different state with a double-peaked resonance. Depending on model and DQD geometry (series or parallel coupled) both a continuous or a discontinuous [6] behavior have been predicted. The quantum transition in the two-impurity Kondo problem has received wide attention in the theoretical literature in the past two decades, to a large extent because the Kondo to AF transition involves an unusual *non-Fermi liquid* fixed point. Experimental investigation of this problem thus far has not been reported.

Here we describe transport properties of an artificial molecule formed by two-path, parallel-coupled double quantum dots, where the interdot tunnel coupling, t, can be tuned. In the Kondo regime the differential conductance, dI/dV, exhibits a single peak centered at zero bias for t comparable to the lead-coupling-induced level broadening. Increasing t by less than 10% resulted in a continuous evolution into a split Kondo resonance. At the same time the conductance at zero bias exhibits a maximum in the vicinity of the transition. This peak splitting behavior in conjunction with distinct temperature dependences in the different regimes demonstrates a direct observation of an interdot-coupling-induced quantum transition. Moreover, on the double-peaked side the zero-bias conductance becomes suppressed; this suppression represents direct evidence that the localized dot spins are becoming entangled into a spin-singlet. While a double-peaked, coherent Kondo effect was observed by Jeong *et al.* in a series-coupled DQD [17], neither the existence of a single-peaked Kondo effect, at finite t, nor spin entanglement was previously established.

The Kondo effect in a single QD results from the coupling between the dot excess (unpaired) spin and the spin of the conduction electrons in the leads. The energy scale is given by the Kondo temperature $T_K \approx \sqrt{U\Gamma}\exp[-\pi|\mu - \epsilon_0|(U + \epsilon_0)/\Gamma U]$ where U is the on-site charging energy, ϵ_0 is the energy of the single-particle level, Γ reflects the dot level broadening from coupling to the leads, and μ is the chemical potential. The fully symmetric DQD system contains the additional parameter, t. The two magnetic impurities, realized by a single excess spin on each dot, interact through an effective AF coupling, $J = 4t^2/U$. The new energy scales, t and J, introduce a rich variety of correlated physics. When U is the dominant energy scale, for energies below U two different scenarios are predicted for dots coupled in series [1–6]. When $t < \Gamma$, the system can be cast [1] into the two-impurity Kondo problem initially discussed by Jones *et al.* [14–16]. The competition between Kondo effect and antiferromagnetism appears as a continuous phase transition (or crossover) at a critical value of the coupling $J/T_K \approx 2.5$. If, however, t is tuned to $t > \Gamma$ before the AF transition point can be reached, the system undergoes a continuous transition from a separate Kondo state of individual spins on each dot (atomiclike) to a coherent bonding-antibonding superposition of the many-body Kondo states of the dots (molecularlike) [2,3,7]. Both the AF state and coherent bonding state exhibit a double-peaked Kondo resonance in the differential conductance versus source-drain bias and involve entanglement of the dot spins into a spin singlet. Therefore, they

are likely closely related. The parallel-coupled case has only recently been analyzed in a model without interdot tunnel coupling where the AF coupling occurs via electrostatic coupling, yielding a discontinuous transition [6].

Our device was fabricated on a $GaAs/Al_xGa_{1-x}As$ heterostructure containing a two-dimensional electron gas 80 nm below the surface, with electron density and mobility of $n = 3.8 \times 10^{11}\ \mathrm{cm}^{-2}$ and $\mu = 9 \times 10^5\ \mathrm{cm}^2/\mathrm{V\,s}$, respectively. The lithographic size of each dot is 170 nm $\times$ 200 nm [see Fig. 1(a)]. The eight separate metallic gates are configured and operated with five independently tunable gate voltages. The dark regions surrounding (and underneath) gates 5 represent 120 nm thick overexposed polymethyl methacrylate (PMMA), which serve as spacer layers to decrease the local capacitance thus preventing depletion, enabling each lead to simultaneously connect to both dots. The experiment was carried out at a lattice temperature of 30 mK. Standard, separate characterization of each dot in the closed dot regime [17] yielded a charging energy U of 2.517 meV (2.95 meV) for the left (right) dot, with corresponding dot-environment capacitance $C_\Sigma \approx 63.6$ aF (54.3 aF), and level spacing $\Delta E \approx 219\ \mu$eV (308 μeV). Modeling the dot as a metal disk embedded in a dielectric resulted in a disk of radius $r_e \approx 70$ nm (60 nm) with 58 (43) electrons. To characterize the DQD device and demonstrate its full tunability, in Fig. 1(b) we show the Coulomb blockade (CB) charging diagram of the conductance versus plunger gates V2 and V4 [18] as t was increased, for weak coupling to the leads where Kondo correlation is unimportant. The central pincher gate V5 controlled t where a reduction of the gate voltage decreased t. At weak coupling (t small), the electrons separately tunnel through the nearly independent dots yielding gridlike rectangular domains in Fig. 1(b)(1). With increasing t charge quantization in each dot is gradually lost as the domain vertices separate and the rectangles deform into rounded hexagons. At large t the two dots merge into one and the domain boundaries become straight lines [Fig. 1(b)(4)]. Such tunability bodes well for quantum computation applications [19].

Γ and t govern the delicate Kondo physics. To obtain the desired large t, the center pincher gate V5 was set so that the zigzag pattern in the charging diagram is barely visible (Fig. 2), ensuring that the Kondo valleys can be located. To form the Kondo states in both dots, pincher gates V1 and V3 were tuned to give a sizable $\Gamma \approx \Delta E$ to ensure strong Kondo correlation. An estimate for t is based on the charging diagram, which indicates a configuration close to the limit of a merged single large dot (Fig. 2), so that the level broadening $\pi|t|^2/\Delta E$ should be comparable to the level spacing ΔE, yielding $t \approx 150\ \mu$eV, while Γ is deduced to be $\approx 150\ \mu$eV from the half-width of the CB peaks.

Care is required when tuning t via V5, while maintaining symmetry between the dots [20]. The mutual capacitive coupling between the gates and dots gives rise to a complex capacitance matrix. Changing V5 simultaneously affected the charge on the dots and other gates. By adjusting the remaining gates, we tuned the Kondo anomaly to be nearly symmetrical about zero bias. We relied mainly on plunger gates V2 or V4, which were found to follow V5 in an approximately linear manner. This procedure can be thought as experimentally diagonalizing the capacitance matrix. The desired configuration of an unpaired excess spin on each dot could be maintained within a V5 tuning range of $\approx$4–7 mV without causing sudden charge reconfiguration. Typically V5 is set $\approx$70 mV above pinchoff. Therefore, the relative tuning range in this Kondo regime is roughly 6%–10% of closure and even smaller for the corresponding fractional change in t, since tunnel coupling becomes exponentially suppressed in the small t limit.

Focusing on the topmost states in each dot, three distinct spin configurations may appear assuming even-odd electron filling (Fig. 2). Our investigation was carried out in such regimes. Non-even-odd behavior was also observable, but will not be discussed [21]. The Kondo valleys and spin states in each dot were identified by measuring the differential conductance, dI/dV, versus source-drain bias, V_{SD}, at an electronic temperature of $\sim$45 mK. For regions 1–6 in Fig. 2, we observed the expected appearance and disappearance of Kondo resonance peaks near zero bias shown in the insets of Fig. 2.

When t was tuned, two distinct regimes of behavior were evident in dI/dV [see Figs. 3(a)–3(e)]. The main

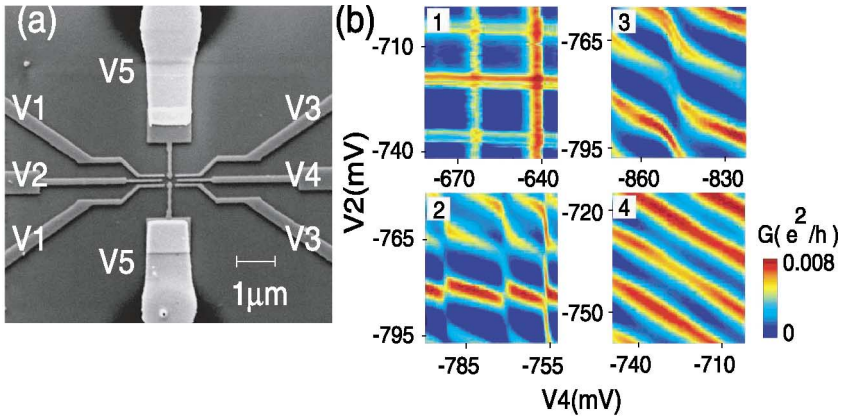

FIG. 1 (color). Device and characterization in the CB regime: (a) Scanning electron micrograph of the device. (b) Logarithm of double dot conductance as a function of gate voltages V2 and V4 for weak lead-dot coupling, first cooldown. The color scale indicates the magnitude of conductance. The voltages in central pincher gate V5 are (1) -0.7477 V, (2) -0.6573 V, (3) -0.6494 V, and (4) -0.5701 V.

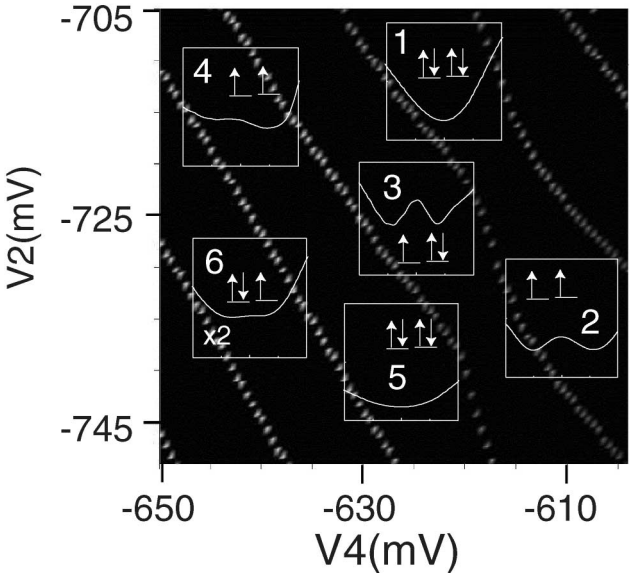

FIG. 2. Device characterization in the Kondo regime: Charging diagram for the third cooldown depicted in a gray-scale plot of the conductance crest as a function of gate voltages V2 and V4 (V5 = −0.5965 V, in the regime shown between Figs. 1(b)(3) and 1(b)(4). The insets indicate the differential conductance traces in different valleys and the spin configuration of the uppermost, occupied electronic levels on each dot. Note that a single upward-pointing arrow denotes only an unpaired electron, and is not intended to represent the actual direction of spin alignment. The x axis of the insets expresses V_{SD} from −0.12 to 0.12 mV, and the y axis presents dI/dV from 0 to $0.3G_0$. In trace 6, y is magnified by 2.

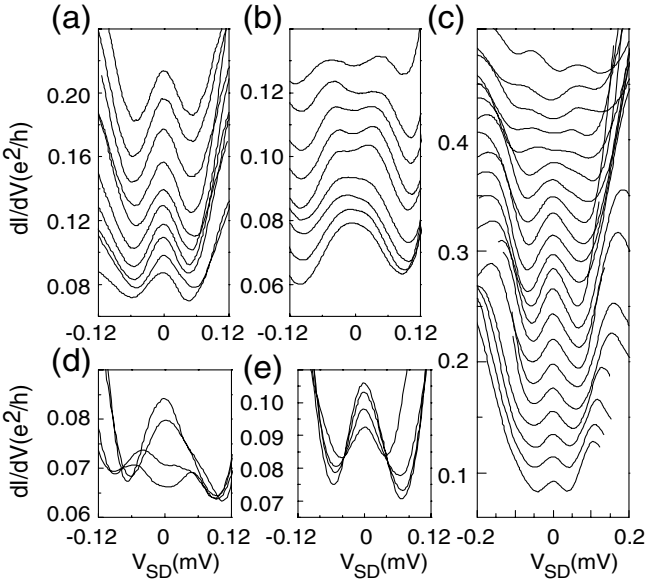

FIG. 3. The differential conductance, dI/dV, versus V_{SD} for different interdot coupling strength tuned via V5 gate. (a) From top to bottom: $V5 = -0.6155V + \Delta V$, $\Delta V = 0, -0.5, -1, -1.5, -2.0, -2.5, -3.0, -3.5, -4.0, -4.5$ mV, second cooldown. (b) From top to bottom: $V5 = -0.5995$ V $+ \Delta V$, $\Delta V = 3.0, 2.5, 2.0, 1.5, 1.7, 1.3, 0.8, 0.3, 0.0$ mV, first cooldown, offset by $0.005e^2/h$ for each trace. (c) From top to bottom: $V5 = -0.5940$ V $+ \Delta V$, $\Delta V = 1.5, 1.2, 0.9, 0.6, 0.3, 0.0, -0.3, -0.6, -0.9, -1.2, -1.5, -1.8, -2.1, -2.4, -2.7, -3.0, -3.3, -3.6, -4.0, -4.3, -4.6$ mV, third cooldown as measured in Kondo valley 2 of Fig. 2, offset by $0.02e^2/h$ for each trace. The traces vary in different cooldowns due to the rearrangement in the occupation of charges in defects and traps. (d),(e) Selected data from (c) without offset. (d) The second quantum state regime (from top to bottom: $V5 = -0.5943, -0.5940, -0.5937, -0.5934$ V). (e) The first quantum state regime (from top to bottom: $V5 = -0.5961, -0.5964, -0.5970, -0.5986$ V).

features in the first regime [see Figs. 3(a) and 3(e)] were the clear presence of a single peak centered at zero bias, an increasing peak width, and an increasing linear conductance $dI/dV|_{V=0}$ with increasing t. Here only the first regime is observable due to a limited tuning range in t. In the second regime where t was increased further [see Figs. 3(b) and 3(d)], the single peak developed into two peaks. In some Kondo valleys, both types of behavior were observed as shown in Figs. 3(c) and 3(d), in which the transition is seen to take place in a continuous manner. In the transition region, the single peak broadened and its zero-bias value approached a maximum and became flat before dropping as the peak gradually split into two. The suppression of the zero-bias conductance on the double-peaked side can be attributed to the emergence of spin-singlet correlation between the two dot spins [1–7]. The maximum $dI/dV|_{V=0}$ is about $\sim 0.1e^2/h$, reduced below the theoretical unitary limit of $4e^2/h$. This reduction can occur when the energy levels in the two dots differ and the dot-lead coupling is asymmetric [3,22].

In Fig. 4 we summarize key parameters deduced from systematic analysis and curve fitting to experimental data [23]. The double-peaked feature visibly disappeared at V5 ~ -0.5943 V as indicated by the dashed line roughly coinciding with the g ($dI/dV|_{V=0}$ above background) maximum position. The peak splitting, $\delta = e\delta V$, dramatically reduces from a maximum of ~ 120 μeV to ~ 0 when V5 is slightly reduced from -0.5925 V to ~ -0.595, and correspondingly t is reduced by less than 4% from an initial value $t \approx 150$ μeV.

In addition to differences in the peak shape, the temperature dependence of dI/dV was also distinct in the two regimes (see Fig. 5). In the first regime, the zero-bias dI/dV, decreased logarithmically with T [Fig. 5(a)]. In contrast, in the second regime, the zero-bias dI/dV exhibited a nonmonotonic behavior [Fig. 5(b)], where with increasing T the zero-bias dI/dV slightly increased initially, then slowly decreased before increasing again when T exceeded T_K. Such behavior was also found in a double peak from Fig. 3(b).

To date no theoretical work has addressed the parallel-coupled DQD with interdot tunnel coupling. Nevertheless, because the Kondo anomaly occurs under slightly nonequilibrium conditions, it is likely that we may identify the observed transition with the quantum critical phenomenon discussed in the two-impurity Kondo problem for the series geometry based on the following evidence: (a) a continuous evolution from the single- to

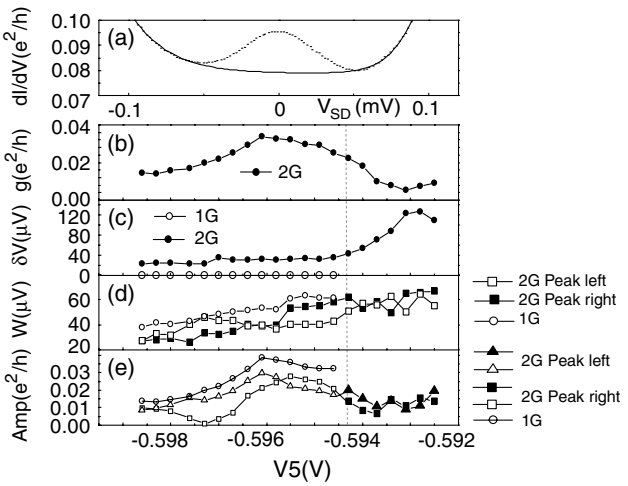

FIG. 4. The linear conductance $g = dI/dV|_{V=0}$ above background, peak splitting δV, width W, and peak amplitude(s) extracted by first subtracting a 2-Boltzmann simulated background ($a_1 + \sum_{i=1}^{2} \frac{a_{i+1}}{1+\exp\{(V_{SD}-X_i)/\alpha_i\}}$) signal followed by a two- or one-Gaussian fit (e.g., two-Gaussian function: $g = \sum_{i=1}^{2} A_i \exp\{-2\frac{(V_{SD}-X_{ci})^2}{W_i^2}\}$) [23]. The data are taken from Fig. 3(c). The fit and data are virtually indistinguishable. (a) Background subtraction. The fitting results are shown in (b)–(e). The double peak feature visibly disappears for V5 $<$ -0.5943 V, marked by the dashed line, where $\delta V \leq W$ and a one-Gaussian fit is equally viable as a two-Gaussian [24].

double-peaked behavior, (b) a maximum in $dI/dV|_{V=0}$ near the transition point, (c) different behaviors in the temperature dependence of the zero-bias conductance, and (d) a strong renormalization of the peak splitting, δ, compared to the estimated t or AF coupling, J, close to the transition (see below). These features are all in qualitative agreement with predictions for a series-coupled DQD [1–7,22], although ideally theory predicts a maximum dI/dV reaching the unitarity limit $4e^2/h$. Semiquantitatively, it is informative to roughly estimate key parameters and compare these to observed splitting, $\delta \lesssim 120$ μeV. Within the theoretical scenarios, δ must be compared to $4t \approx 600$ μeV or $2J = 8t^2/U \approx$ 180 μeV. (Note that in the open dot regime U is expected to be reduced from its closed dot value by roughly 1/3 [11], yielding $U \approx 1$ meV.) The reduction of δ compared to $4t$ and $2J$ is in agreement with theory and lends further credibility to our identification of the quantum transition.

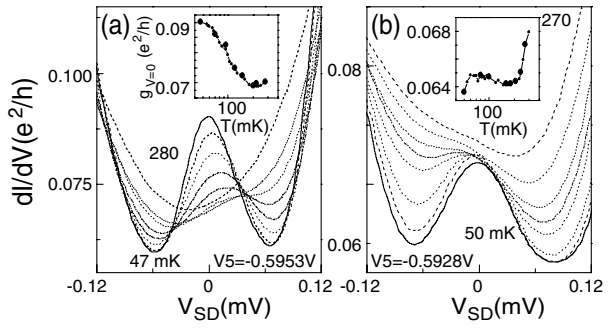

FIG. 5. Temperature dependence of dI/dV versus V_{SD} within the Kondo valley of Fig. 3(c) at slightly displaced voltage settings: (a) First quantum state regime. (b) Second regime near the transition point. Insets: $dI/dV|_{V=0} \equiv g_{V=0}$ versus T (large dots are from curves shown).

We thank H. Baranger, K. Matveev, S. Khlebnikov, N. Giordano, N. Wingreen, D. Cox, A. Schiller, and H. Nakanishi for discussions, and F. Altomare, L. C. Tung, V. Gusiatnikov, and H. Jeong for assistance in the experiment. This work was supported by NSF Grants No. DMR-9801760 and No. DMR-0135931.

*Current address: Department of Physics, Duke University, Durham, NC 27708, USA.

[1] A. Georges and Y. Meir, Phys. Rev. Lett. **82**, 3508 (1999).
[2] R. Aguado and D. C. Langreth, Phys. Rev. Lett. **85**, 1946 (2000).
[3] T. Aono and M. Eto, Phys. Rev. B **63**, 125327 (2001).
[4] B. Dong and L. L. Lei, Phys. Rev. B **65**, 241304 (2002).
[5] W. Izumida and O. Sakai, Phys. Rev. B **62**, 10260 (2000).
[6] R. López *et al.*, Phys. Rev. Lett. **89**, 136802 (2002).
[7] C. A. Büsser *et al.*, Phys. Rev. B **62**, 9907 (2000).
[8] D. Goldhaber-Gordon *et al.*, Nature (London) **391**, 156 (1998).
[9] S. M. Cronenwett *et al.*, Science **281**, 540 (1998).
[10] S. Sasaki *et al.*, Nature (London) **405**, 764 (2000).
[11] W. G. van der Wiel *et al.*, Science **289**, 2105 (2000).
[12] Y. Ji *et al.*, Science **290**, 779 (2000).
[13] J. Nygard *et al.*, Nature (London) **408**, 342 (2000).
[14] B. A. Jones and C. M. Varma, Phys. Rev. Lett. **58**, 843 (1987).
[15] B. A. Jones *et al.*, Phys. Rev. Lett. **61**, 125 (1988).
[16] I. Affleck and A. W. W. Ludwig, Phys. Rev. Lett. **68**, 1046 (1992).
[17] H. Jeong, A. M. Chang, and M. R. Melloch, Science **293**, 2221 (2001).
[18] C. Livermore *et al.*, Science **274**, 1332 (1996).
[19] D. Loss and D. P. DiVincenzo, Phys. Rev. A **57**, 120 (1998).
[20] F. Simmel *et al.*, Phys. Rev. Lett. **83**, 804 (1999).
[21] J. Schmid *et al.*, Phys. Rev. Lett. **84**, 5824 (2000).
[22] R. Aguado and D. C. Langreth, Phys. Rev. B **67**, 245307 (2003).
[23] J.C. Chen and A.M. Chang, EPAPS Document No. E-PRLTAO-92-051413. This EPAPS supplementary document contains a detailed description of the data analysis and curve fitting procedure. In addition, figures summarizing the fitting parameters, e.g., the zero-bias differential conductance, the peak splitting, and peak widths are presented. The analysis is useful in establishing the main conclusions presented in this Letter. A direct link to this document may be found in the online article's HTML reference section. The document may also be reached via the EPAPS homepage (http://www.aip.org/pubservs/epaps.html) or from ftp.aip.org in the directory /epaps/. See the EPAPS homepage for more information.
[24] When $\delta V \leq W$, the two-Gaussian amplitudes A_1 and A_2 become sensitive to residual asymmetries left after background subtraction, as well as to the peak shape.